Encapsulation of Thymol in cyclodextrin nano-cavities: A multi spectroscopic and theoretical study

Adity Bose[1]*, Priti Sengupta[1] , Uttam Pal[2], Sanib Senapati[3], Mohd. Ahsan[3], Santanu Roy[4], Upasana Das[4], Kamalika Sen[5]

[1]Department of Chemistry, Presidency University, 86/1 College Street, Kolkata 700073, West Bengal, India.

[2]Chemical Sciences Division, Saha Institute of Nuclear Physics, Block AF, Saltlake, Kolkata 700064, West Bengal, India.

[3]Department of Biotechnology, Indian Institute of Technology, Madras, IIT P.O., Chennai 600 036, India.

[4]Department of Microbiology, Acharya Prafulla Chandra College, New Barrackpore, Kolkata 700131, India.

[5]Department of Chemistry, University of Calcutta, 92, A. P. C. Road, Kolkata 700 009, India.

Correspondence:

- **Email: adity.chem@presiuniv.ac.in, adityc17j@gmail.com**

Abstract:

Cyclodextrins have a wide range of applications in different areas of drug delivery and pharmaceutical industry due to their complexation ability and other versatile characteristics. Here we have studied the binding interactions of a small biologically important phenolic molecule, Thymol (Th), with both α and β cyclodextrins (CDs), which are well known drug delivery vehicles. Extent of encapsulation has been determined using several spectroscopic techniques. In fluorescence experiments, significant increase in fluorescence intensities have been discerned for both the CDs but there had been a much early saturation for αCD. Anisotropy experiments have been performed too and very surprisingly no appreciable increase in anisotropy value was observed in either case. Isothermal titration calorimetry (ITC) data, however, show signature of binding of Th with the βCD. These intriguing results were explained with the help of molecular docking and dynamics simulation studies. The docking calculations have shown that Th goes inside both α and βCD. In keeping with the final NMR data and molecular dynamics we have ultimately concluded that solvated Th molecules are the main participants in the interaction with CDs which is responsible for these intriguing behaviors. Finally we have also performed an antioxidant assay to reveal the practical application of such encapsulation. It has been found that on encapsulation there is an enhancement of the antioxidant behavior of Th. Then we have also performed an antibacterial assay to show the unchanged antibacterial properties of Th on encapsulation. Hence it can be deduced that Th can be safely delivered through CDs in living system without hampering its beneficial properties.

Keywords:

Thymol; Cyclodextrin; fluorescence; NMR; molecular dynamics; antimicrobial assay.

1. Introduction:

Cyclodextrins (CDs) are toroidally shaped polysaccharides made up of six to eight d-glucose monomers connected at the 1 and 4 carbon atoms. The cavities of CDs are relatively hydrophobic and have an internal diameter of 4.7–8.3Å.[1,2] This difference in cavity size allows binding specificity to be tailored based on substrate size and geometry. In an aqueous environment, CDs form inclusion complexes with many lipophilic drug molecules through a process in which water molecules located inside the central cavity are replaced by some lipophilic structure of the drug molecule. Therefore, CDs are ideal molecules for the study of small molecule binding. The different cavity widths of α- and βCDs in combination with substrates of different size, polarity and polarizibility offer a unique opportunity to study the change in binding mechanisms in aqueous solutions, presenting geometrically well-defined models for many biologically important complexes.

There are many studies dealing with inclusion complexes of CDs.[3–8] The structure of a supramolecule consisting of CD as a host and organic molecule along with several solvent molecules as guests is quite well defined.[9] It is generally accepted that CD can form inclusion complex in aqueous solution where a lipophilic guest molecule or moiety locates in the inner cavity. Due to this special property, CDs have been used extensively in pharmaceutical research as it increases solubility of drugs, reduces bitterness, enhances stability and decreases tissue irritation.[10] Worldwide, different pharmaceutical products containing CDs have already reached the market.[11]

We have been working for some time on Thymol (Th) which has antimicrobial, antibacterial and antioxidant activity because of its phenolic structure.[12, 13] We are mainly interested to understand the mode of behavior of this molecule as a model drug and hence our endeavor to study its behavior with the drug delivery vehicle CD. We have performed UV-Vis absorption, steady state fluorescence, fluorescence lifetime, fluorescence anisotropy, ITC, NMR and computational studies to comprehend the behavioral pattern of the molecules during encapsulation. The culmination of all data suggested a very important phenomenon. Th, a photoacid remains in its conjugate base form in the neutral pH used in our studies.[14] So, its chance of being hydrated with neighbouring water molecules is significant. This results in an overall increase in its size. Now, as the molecule is subjected to the presence of CDs, it tries to get encapsulated in the hydrophobic core. βCD molecule having a larger core cavity encourages the solvated Th molecule to enter with ease, resulting in an increase in fluorescence intensity, but again due to solvation, the expected increase in anisotropy is not observed. ITC and NMR data also points to the encapsulation of the Th molecule in βCD. In comparison results with αCD is a bit dubious. Fluorescence enhancement has been observed initially only but NMR data speaks against such encapsulation.

However, molecular docking calculations assert that βCD can easily engulf a Th molecule. In contrast, in presence of αCD the bulkier Th molecule fails to get properly encapsulated in the core, resulting in a small increase in Th fluorescence intensity only initially on addition of increasing amounts of αCD. The scope of Th to enter the cavity of α-CD is appreciable when it is not hydrated as pointed out by the docking calculations. But from molecular dynamics simulation studies it is very much evident that a hydrated Th is

not comfortable in αCD cavity and flies off. Understanding the mode of interaction of Th with both CDs, our next endeavor was to assess the effect of encapsulation on the beneficial roles of Th such as antioxidant and antibacterial properties. We have performed a DPPH antioxidant assay of Th with βCD, where an increase in antioxidant behavior has been discerned on encapsulation. Further we have performed an antibacterial assay and found an unaltered effect on encapsulation. Thus Th delivery within CD cavity can be a promising tool in future.

2. Materials and Methods:

2.1. Materials:

Thymol (structure 1) was purchased from Merck chemicals. Both α and βCDs were purchased from Sigma Aldrich. 2,2-diphenyl-2-picrylhydrazyl (DPPH) was purchased from SRL, India. Methanol and dimethyl sulfoxide (DMSO) were purchased from Merck. Thymol solution was made in warm water. The water used in all the experiments is double distilled. ^{1}H-NMR data were taken in D_2O, which was purchased from Sigma Aldrich. All the samples during NMR studies were dissolved in D_2O.

Bacillus subtilis was used as the test organism in the antimicrobial assay. To prepare the sets for biological assay (antimicrobial assay), thymol was dissolved in 2.5% (v/v) DMSO in sterile distilled water and working concentration was 50 mg/ml. The stock solution of αCD and βCD were prepared using sterile distilled water. The sets of Th-αCD and Th-βCD were prepared by maintaining equal concentration of both the components to satisfy 1:1 binding

stoichiometry. All the solutions were prepared in laminar flow cabinet with proper precautions to avoid any bacterial interference.

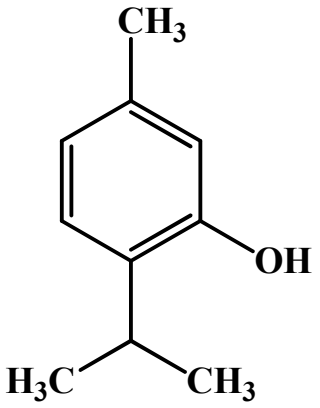

Structure 1. Chemical Structure of Thymol (Th)

2.2. Methods:

2.2.1. Absorption and Steady State Fluorescence Measurements

UV-vis absorption spectra were recorded on a Hitachi U-4100 spectrophotometer at 298 K. The steady state fluorescence measurements at an excitation of 275 nm was made in a Hitachi F-7000 spectrofluorimeter (equipped with a 150 W xenon lamp) using a 1 cm path length quartz cuvette. All the measurements at 298 K were made by exciting the samples at 275 nm using 5 nm band-passes for excitation and emission both using the correct mode of the instrument. Inner filter effects have been eliminated in all the emission spectra.

For the fluorescence titration experiments 50 μM Th was taken in the cuvette and the α or βCD concentration was varied from 0 to 750 μM or 1000 μM, respectively. The

formation constant (K) of the CD:Th complex has been determined using Benesi–Hildebrand relation.[15]

$$\frac{1}{(F_i - F_0)} = \frac{1}{(F_{max} - F_0) \times K_a \times [CD]^n} + \frac{1}{(F_{max} - F_0)} \quad \text{(Eq. 1)}$$

where, F_i and F_0 stands for the fluorescence value of Th on addition of CD and free Th respectively. F_{max} is the saturation fluorescence value and k_a is the formation constant of the inclusion complex which is the ratio of intercept to slope and n is the binding stoichiometry of CD to Th.

2.2.2. Fluorescence Anisotropy Measurements

The steady-state fluorescence anisotropy measurements were made in a Varian Cary Eclipse spectrofluorimeter using a 1 cm path length quartz cuvette at 298 K. During the steady-state fluorescence studies, samples were excited at 275 nm. The steady-state anisotropy, r is defined by:[16]

$$r = I_{VV} - GI_{VH} / I_{VV} + 2GI_{VH} \quad \text{(Eq. 2)}$$

where I_{VV} and I_{VH} are the emission intensities obtained with the excitation polarizer oriented vertically and emission polarizer oriented vertically and horizontally, respectively. The G factor is defined as: $G=I_{HV}/I_{HH,}$ where the intensities I_{HV} and I_{HH} refer to the vertical and horizontal positions of the emission polarizer, with the excitation polarizer being horizontal.

2.2.3. Time Resolved Emission Measurements

Singlet state lifetime (τ) was measured by Time Master fluorimeter from Photon Technology International (PTI, U.S.). The system consists of a pulsed laser driver of a PDL series i.e., PDL- 800-B (from Picoquant, Germany) with interchangeable sub nano second pulsed LEDs and pico-diode lasers (Picoquant, Germany) with a TCSPC set up (PTI, U.S.). The software Felix 32 controls all acquisition modes and data analysis of the Time Master system. Decay measurements using "magic angle" detection with an emission polarizer set at 55° were carried out and no detectable difference in the fitted τ values with those obtained from normal decay measurements were observed. The samples were excited using PLS-280 (Pulse Width-700 ps) at a repetition frequency 10 MHz. Instrument response functions (IRF) were measured at the respective excitation wavelengths, namely, 280 nm using slits with a band-pass of 5 nm using Ludox as the scatterer. The decay of sample was analyzed by a nonlinear iterative fitting procedure based on the Marquardt algorithm. The deconvolution technique used can determine the lifetime up to 200 ps with sub nano second pulsed LEDs. The quality of fit has been assessed over the entire decay, including the rising edge, and tested with a plot of weighted residuals and other statistical parameters, for example, the reduced χ^2 ratio and the Durbin- Watson (DW) parameters. Average fluorescence lifetimes ($<\tau>$) for bi-exponential iterative fittings were evaluated from the decay components and the normalized pre-exponential factors using the following relation:

$$<\tau> = \alpha_1\tau_1 + \alpha_2\tau_2 \qquad \text{(Eq. 3)}$$

2.2.4. Isothermal titration calorimetry (ITC)

Isothermal titration calorimetry experiments were performed in a Microcal-ITC_{200} calorimeter (MicroCal Inc., USA) using the built in VP viewer 2000 software with Origin 7.0. All experiments were performed at a fixed temperature of (298.2±0.1) K and repeated thrice.

2.2.5. ^1H NMR measurements

^1H NMR spectra were recorded on a 300 MHz Bruker Nuclear Magnetic Resonance Instrument, using tetramethylsilane as an internal standard. All the experiments were recorded using D_2O as solvent. The solutions were transferred in 5 mm NMR tubes, giving a sample total volume of 500 uL. The probe temperature was regulated at 298 K.

2.2.6. Molecular Docking

Crystal structure of α and βCD was obtained from Cambridge crystallographic data centre. Crystal structures with reference code BAJJAX and POBRON were used for α and βCD, respectively. The αCD crystal structure contained a small molecule ligand, while βCD had crystal water in the cavity. The ligand/water were removed from the CD structures to obtain the apo form of the receptor. Subsequently, the CD structures were optimized by quantum mechanical calculations, using Gaussian 09 program with HF/sto-3g level of theory. The ligand of interest, thymol was built and optimized quantum mechanically with MP2/6-31g** level of theory.

Auto Dock Tools (version 1.5.6) was used for CD-Th docking studies. Autodock is one of the most widely used tools to study the receptor-ligand binding and to compute

binding energy. Grid box in the receptor was prepared using autogrid tool in AutoDock, with the grid box size of (10.5×10.5 ×10.5) cubic Å and (12×12×12) cubic Å for α and βCD, respectively, such that the whole receptor molecule was covered for docking. Grid point spacing of 0.375 Å was used. Conformational sampling for receptor-ligand docking was done using Lamarckian genetic algorithm.

2.2.7. Molecular Dynamics

Both the docked complexes as obtained from docking were subjected to molecular dynamics (MD) simulations using Desmond[17] as implemented in Schrodinger Maestro (Academic version 2016-4). MD was run for 48 ns in SPC (single point charge) water environment under optimized potentials for liquid simulations, OPLS 2005, forcefield.[18] Five step relaxation protocol was used before the production MD as described in earlier studies.[19] Root mean square deviation (RMSD) and hydrogen bond calculations were performed on the MD trajectory using the simulation event analysis tool in Schrodinger Maestro.

2.2.8. Radical Scavenging assay

The DPPH (2,2-diphenyl-1-picrylhydrazyl) radical scavenging activity was determined according to the method of Shimada, Fujikawa, Yahara and Nakamura.[20] The sample was dissolved in water to prepare various concentrations of Th, 0-3.5 mM. 0.5 mL of sample solution of different concentration was mixed with 3 mL of 0.1 mM DPPH in

methanol. The mixture was mixed properly and maintained for 20 min in dark. The absorbance was measured at 517 nm. The absorbance of the control was obtained by replacing the sample with water. The scavenging activity was calculated using the following equation:

Radical Scavenging activity (%)

= (A_{517} of control - A_{517} of sample of different concentration)/ A_{517} of control X 100 (Eq.4)

2.2.9. Antimicrobial assay

The *B*. *subtilis* was initially grown overnight (16 hr) at 37 °C, with vigorous shaking, in nutrient broth medium (beef extract 3 $g.L^{-1}$, peptone 5 $g.L^{-1}$). The cells were diluted with sterile nutrient broth to 0.5 McFarland standard (~10^8 $CFU.mL^{-1}$) and swabbed onto Mueller Hinton agar plates[21] with a media thickness of 4 mm.[22] Six cups with 7 mm diameter were bored in the agar and 50 µL of the following, prepared as stated above, were added in them: free Th, Th with αCD, Th with βCD, free αCD, free βCD and 2.5% (v/v) DMSO in sterile distilled water (as a negative control). The plates were initially incubated for 24 hr and then for a further 24 hr (total 48 hr) at 37 °C. They were checked for the appearance of clear zones surrounding the cups after 24 hr and 48 hr.

3. Results and discussion:

3.1. Absorption spectral studies

Spectrophotometric analysis was carried out to determine the molecular encapsulation behavior of CDs with Th in aqueous solution. The absorption spectral data of

Th with different concentration of CDs is given in Fig. 1. On increasing the concentration of βCD, it is observed that there is a negligible change in the peak position and intensity. Hence, we could conclude that interaction with Th is not much affected in ground state. Similar phenomenon was observed with αCD, as well (data not shown).

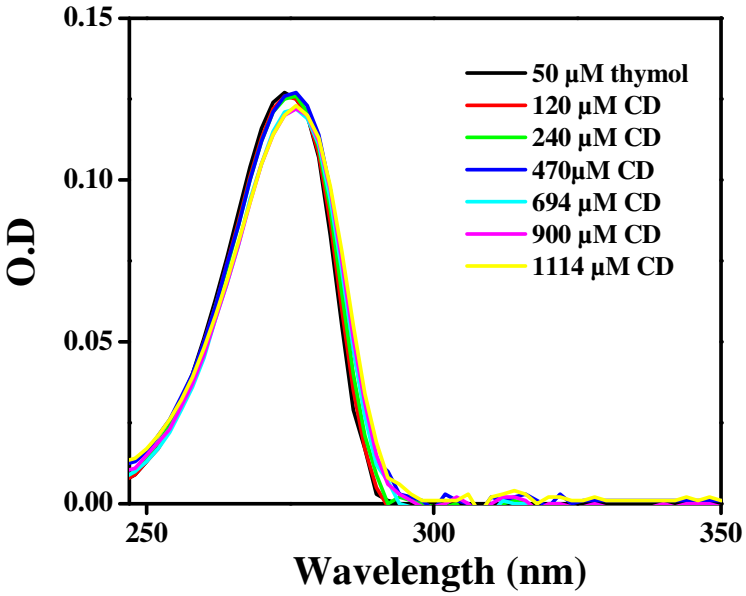

Fig. 1. Absorption spectra of Th with increasing concentration of βCD in aqueous medium.

3.2. Fluorescence spectral studies

The fluorescence emission spectral data of Th with different concentrations of βCD is given in Fig. 2. The effects of βCD on the emission spectra of Th are more pronounced than the corresponding effect on the absorption spectra with respect to the concentration of βCD. From this figure, it is observed that fluorescence signal increases with increasing concentration of βCD but there was no apparent shifting in the fluorescence maxima. The

results suggest that a stable inclusion complex is formed between Th and βCD without any apparent change in the hydrophobicity around Th. The increase in fluorescence intensity while increasing βCD concentration during the formation of inclusion complex may be due to lowering of solvent polarity provided by βCD cavity.[23]

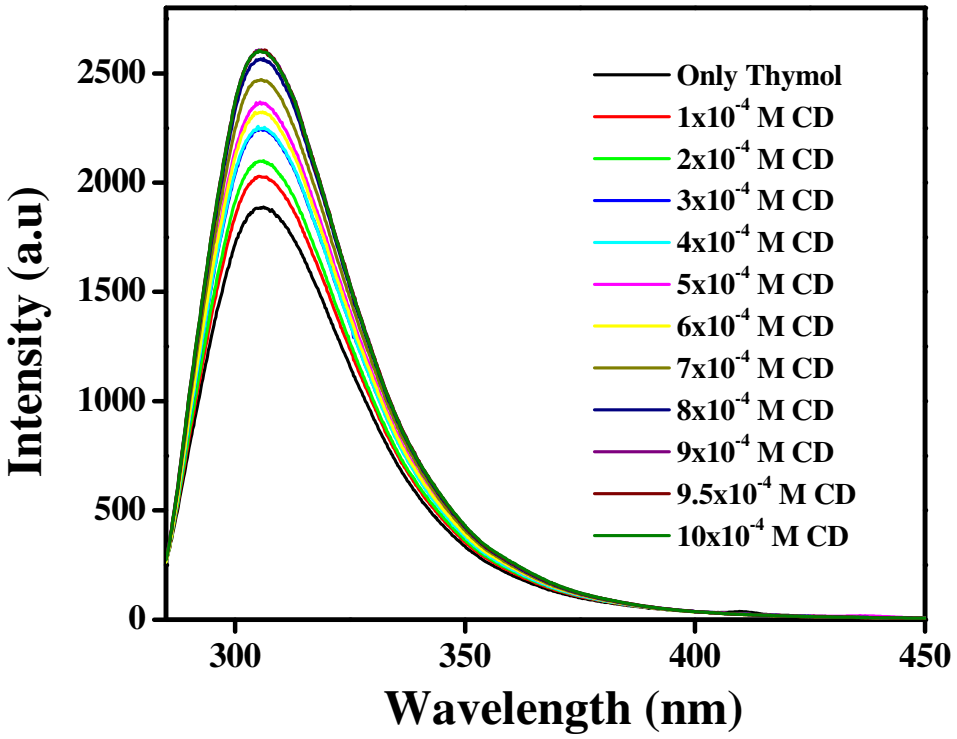

Fig. 2. Fluorescence spectra of Th (50 μM) with increasing concentration of βCD

Fig. 3 depicts the pattern of increasing concentration of αCD on fluorescence emission of Th. From the figure it is evident that there is only an initial increment of fluorescence signal on addition of αCD (upto 375 uM). After that there is a steady decrease. This observation is

in contrary to the one obtained from βCD and can only be associated to the cavity size difference among the CDs.

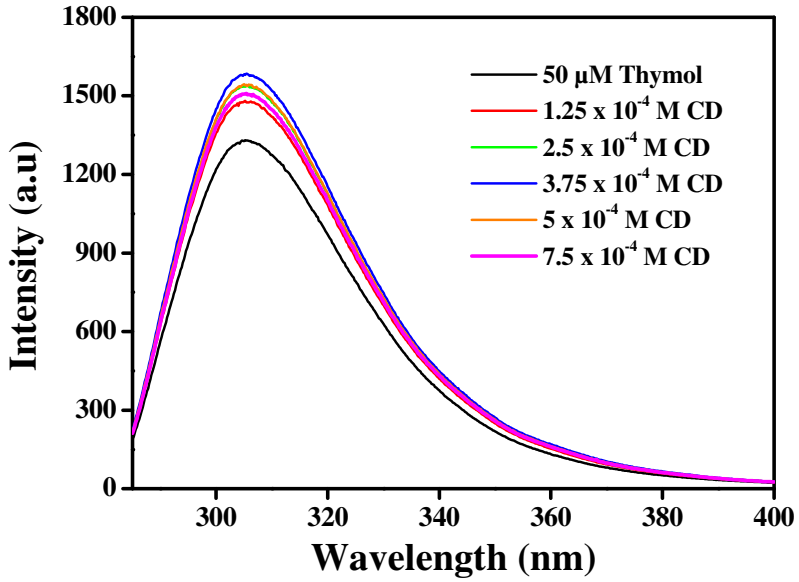

Fig. 3. Fluorescence spectra of Th with increasing concentration of αCD

The formation constant (K) of the βCD:Th complex has been determined using Benesi–Hildebrand relation (Eq. 1). A good linear regression (R^2= 0.9918) was obtained when $1/(F_i - F_0)$ is plotted against 1/[CD] (Fig. 4). The linearity of the plot reveals that the stoichiometry of the complex between Th and βCD is 1:1. Whereas a non-linear relationship is obtained when $1/F_i - F_0$ is plotted against$1/[CD]^2$ (inset of fig. 4). The non-linearity of the plot ruled out the

possibility of 1:2 stoichiometry between Th and βCD. From the plot, the formation constant was found to be 2.3 x 10^3 M^{-1} at 298K. The resulting equilibrium can be written as,

$$Th + \beta CD \rightleftharpoons Th: \beta CD \qquad \text{(Eq. 5)}$$

where, Th:βCD, represents the 1:1 inclusion complex of βCD and Th respectively.

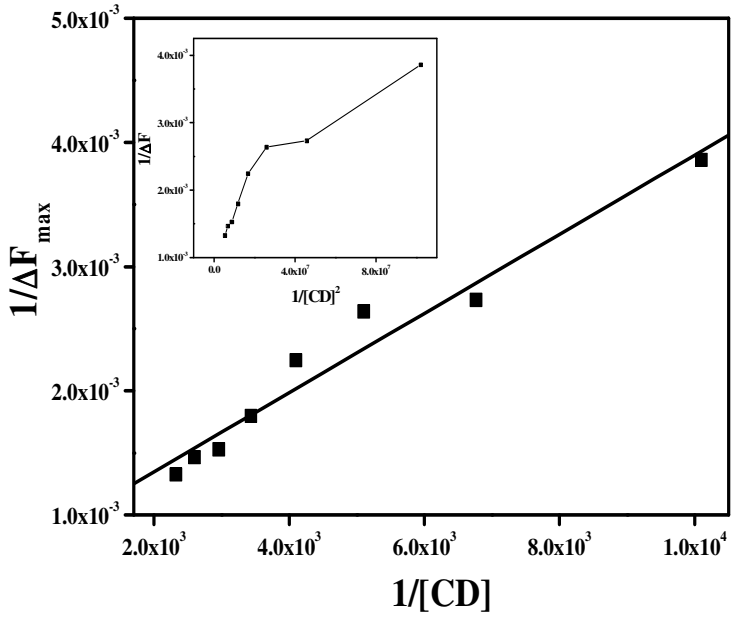

Fig. 4. Benesi–Hildebrand plot of $1/(F_i - F_0)$ against 1/[CD] for Th with βCD (λ_{max}= 310 nm). Inset: Benesi–Hildebrand plot of $1/(F_i - F_0)$ against $1/[CD]^2$ for Th with βCD (λ_{max}= 310 nm).

3.3. Lifetime measurements:

Fluorescence lifetime measurements serve as a sensitive indicator for monitoring excited state affairs of a fluorophore. Hence, the measurements of the emission decays of

Th at different concentrations of βCD complement the ensuing spectroscopic investigations. The typical time-resolved fluorescence decay profile is presented in fig. 5 with the corresponding decay parameters being summarized in table 1.

Table 1. Singlet State lifetime of Th as a function of added concentration of βCD with λ_{ex} = 280 nm at 298 K.

System	Singlet state lifetime (ns)				
	single exp	Bi-exp			
	τ	τ_1	τ_2	τ_{av}	χ^2
Free Th	1.84 (χ^2 = 1.34)	1.627 (89.21%)	3.722 (10.79%)	1.853	1.002
+ 0.18 mM βCD	----------	1.582 (77.08%)	3.864 (22.92%)	2.105	0.97
+ 0.36 mM βCD	----------	1.623 (66.56%)	3.908 (33.44%)	2.387	1.161
+ 0.54 mM βCD	----------	1.73 (61.5%)	4.001 (38.5%)	2.604	1.248
+ 0.90 mM βCD	----------	1.536 (44.94%)	3.816 (55.06%)	2.791	1.213

Initially, at zero concentrations of βCD the fluorescence decays of the Th are found to be simple, and could be analysed using a single exponential decay equation also. However, at higher concentrations of βCD the fluorescence decays got modified and could be analysed by a biexponential decay equation. Such behaviour may be attributed to the existence of two kinds of fluorescent species, firstly the free fluorophore in aqueous phase (τ_1), and secondly the fluorophore complexed with βCD (τ_2).[16] The average lifetimes have been judged as an authentic parameter for exploring the excited state behaviour of Th at

different concentrations of βCD, rather than emphasizing on the magnitude of individual decay time constants of the bi-exponential decay.

Addition of 0.18 mM βCD enhances the average fluorescence lifetime of Th from 1.85 to 2.105 ns and it is gradually increased on addition of βCD. Fluorescence lifetimes are enhanced with increase in concentrations of βCD due to the accumulation of complexed probes. The complexed probes have higher fluorescence lifetime owing to the diminution of nonradiative decay channels upon complex formation. Again flexible motion of the guest is expected to reduce largely on forming inclusion complexes (i.e., confinement of probe) with the hosts, and hence, fluorescence decay time is expected to be increased. An increase in decay time suggests an increase of rigidity of the guest molecule on interaction with the supramolecular host molecule.[24] This can also be concluded from the increase in τ_2 value (both in magnitude and percentage of the component).

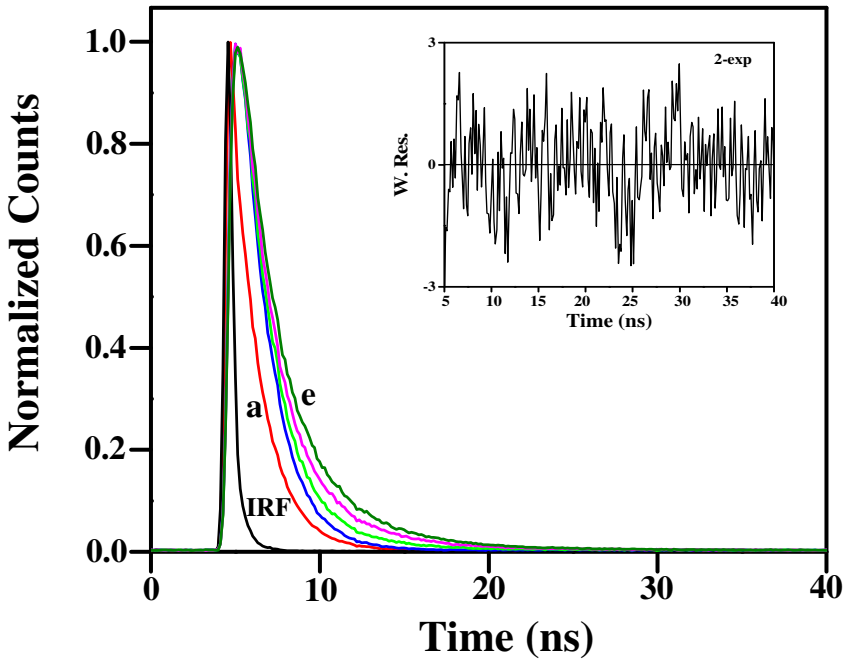

Fig. 5. Typical time-resolved fluorescence decay profiles of Thymol with increasing concentration of βCD (λ_{em} = 310 nm in water); a = Free thymol; a-e: 0.0, 0.18, 0.36, 0.54 and 0.90 mM βCD.

In contrast, the addition of αCD to Th, gives almost a negligible increase in the lifetime value, as given in table 2 and fig. 6. Thus based on the above discussion it can be deduced that the entry of Th molecule within αCD is restricted. Further experimental and theoretical works were performed to have a better understanding.

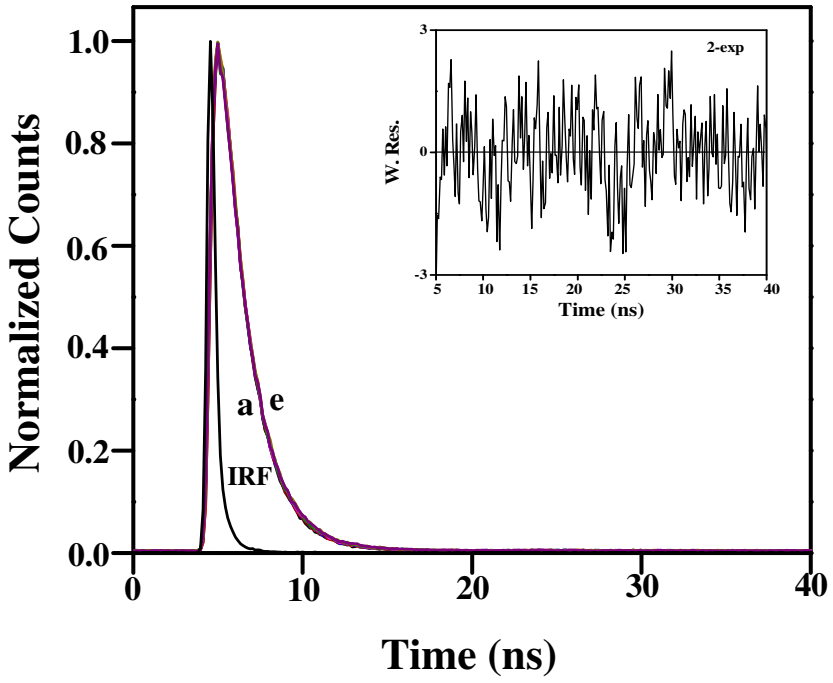

Fig. 6. Typical time-resolved fluorescence decay profiles of Thymol with increasing concentration of αCD (λ_{em} = 310 nm in water); a = Free thymol; a-e: 0.0, 0.18, 0.36, 0.54 and 0.90 mM αCD.

Table 2. Singlet state lifetime of Th as a function of added concentration of αCD with λ_{ex} = 280 nm at 298 K.

System	Singlet state lifetime (ns)				
	single exp	Bi-exp			
	τ	τ_1 (%α_1)	τ_2 (%α_2)	τ_{avg}	χ^2
Free Th	1.62 (χ^2 = 1.34)	1.627 (89.21%)	2.722 (10.79%)	1.653	1.002
+ 0.18 mM αCD	1.624 (χ^2 = 1.152)	1.607 (99.7%)	6.24 (0.22%)	1.617	0.95
+ 0.36 mM αCD	1.64 (χ^2 = 1.192)	1.63 (99.91%)	39.79 (0.088%)	1.644	1.074
+ 0.54 mM αCD	1.647 (χ^2 = 1.36)	1.626 (99.87%)	14.39 (0.128 %)	1.642	1.11
+ 0.90 mM αCD	1.65 (χ^2 = 1.43)	1.604 (99.27%)	4.521 (0.73%)	1.626	1.116

3.4. Isothermal titration calorimetry:

To gain an insight into the thermodynamics of interaction of Th with βCD we resort to isothermal titration calorimetry, which is the most direct method to measure the heat change at a constant temperature. The interaction between a drug and a biomolecule may involve hydrophobic forces, electrostatic interactions, van der Waals interactions, hydrogen bonds, etc. Thermodynamic parameters, free energy changes (ΔG), enthalpy changes (ΔH) and entropy changes (ΔS) of interactions are essential to interpret the binding mode.

The sign and magnitude of the thermodynamic parameter associated with various individual kinds of interaction which may take place in the protein association processes

were judicially characterized by Ross et al.[25] The negative sign for ΔG means that the interaction process is spontaneous. The negative ΔH and negative ΔS indicate that van der Waals interaction and hydrogen bonding play a major role in the binding.

ITC experiment also confirmed the occurrence of a 1:1 binding of Th to βCD as suggested by spectroscopic techniques. The values of formation constants and thermodynamic parameters determined by ITC (Fig. 7) are as follows: n = 1, K = 2.10 X 10^3 M^{-1}, ΔH = -3.19 kcal/mol and ΔS = -73.9 cal mol^{-1} K^{-1}. This again points towards a favourable encapsulation within βCD. Similar experiments with αCD did not produce suitable data and hence are omitted.

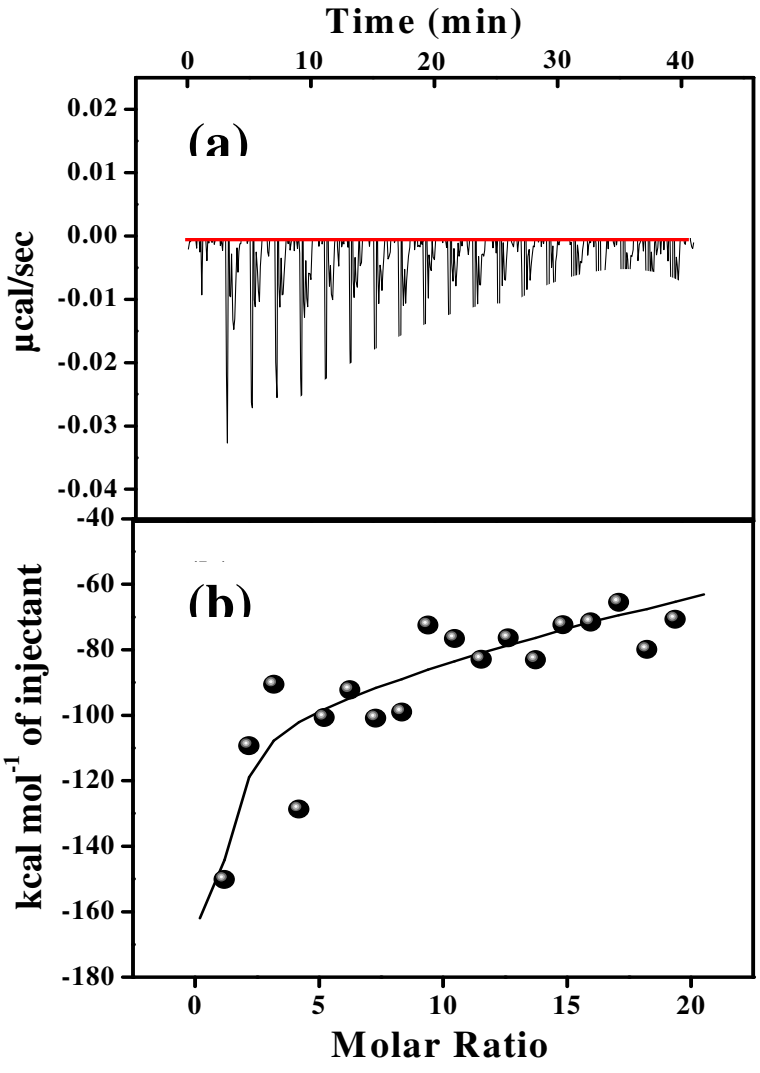

Fig. 7. (a) ITC isotherm for the injection of 25 μM Th solution containing 400 μM βCD at 298 K, following removal of the heat of dilution; (b) data points show integrated heats of interaction as a function of molar ratio and the solid line represents the line of best fit obtained.

Thus encapsulation of Th within βCD has been found to be favoured by H bonding and van der Waals interaction. Further support to this phenomenon has been found from molecular dynamics studies.

3.5. Steady state anisotropy measurements

Steady state fluorescence anisotropy measurements have also been performed since it is generally used to confirm formation of inclusion complexes between the hosts and guest. Since encapsulation of any molecule in the micropockets of βCD imposes motional restriction of the probe, this study can be a useful tool to assess the probable location of the probe in these supramolecular assemblies. An increase in rotational anisotropy upon CD addition is a signature of an increase in motional restriction of the fluorophore on getting encapsulated. Encapsulation generally results in the rigidity of the neighbouring environment of a fluorophore. Fig. 8 shows the variation of steady state anisotropy with increasing concentration of βCD while the inset of fig. 8 shows the variation of steady state anisotropy with increasing concentration of αCD.

Surprisingly in case of βCD, there has been a steady decrease in the anisotropy values while in the smaller αCD there had been a very negligible increase. The observation with βCD had been quite contrary to the steady state and time resolved fluorescence data where an increase in fluorescence intensity and lifetime was evidenced pointing towards

encapsulation which should have resulted in an increase in the rotational anisotropy value. For a further understanding of this anomaly, we have performed NMR and theoretical modelling studies.

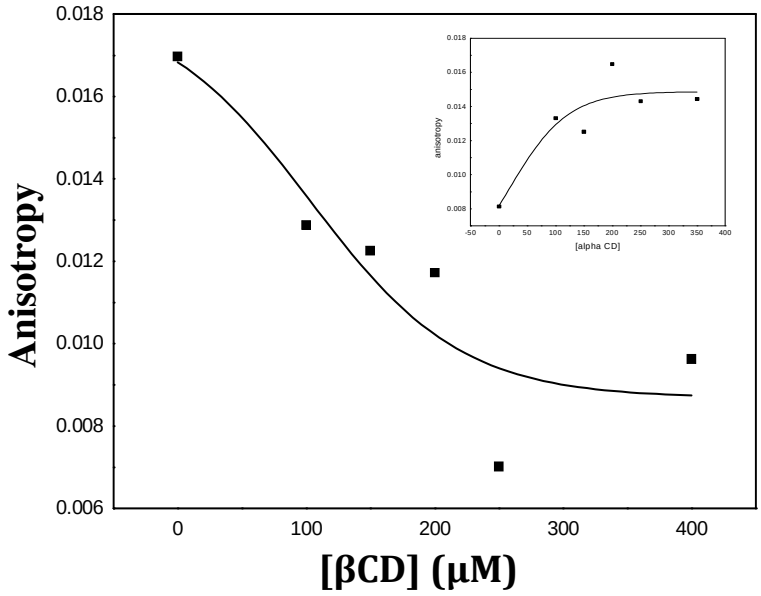

Fig. 8. Variation of steady-state fluorescence anisotropy (r) Th with added βCD. Inset: Variation of steady-state fluorescence anisotropy (r) Th with added αCD.

3.6. ^{1}H NMR studies on the host–guest complex:

Since ^{1}H NMR spectroscopy was first introduced for the study of complex formation in aqueous solutions, there have been numerous studies involving aromatic compounds.[26,27] The method relies on changes in chemical shifts caused by the guest and the host on each other. In the case of aromatic compounds, some of the most important

spectral changes that occur upon complexation come from the diamagnetic shielding of the aromatic host on the nearby spins of the guest.

After the addition of Th in βCD solution, position of protons shifted. H_D proton of Th was slightly upfield shifted from 7.068 to 6.965 ppm. Also the H_E and H_F protons of thymol were shifted upfield from 6.692 to 6.570 and from 6.612 to 6.587, respectively. This clearly indicates that βCD environment affects the aromatic protons of the Th moiety. This was further confirmed by the shifting of the βCD protons due to the addition of Th. H_a of βCD was shifted towards upfield from 4.929 to 4.883 ppm. H_d protons were shifted from 3.820 to 3.747 ppm and H_b protons were highly upfield shifted from 3.732 to 3.589 ppm. From the NMR titration we can conclude that the aromatic ring along with $-CH_3$, is inside the β-CD cavity and the $-CH(CH_3)$ group is outside the cavity as there is no change in ppm values.

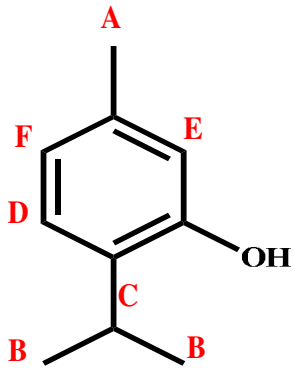

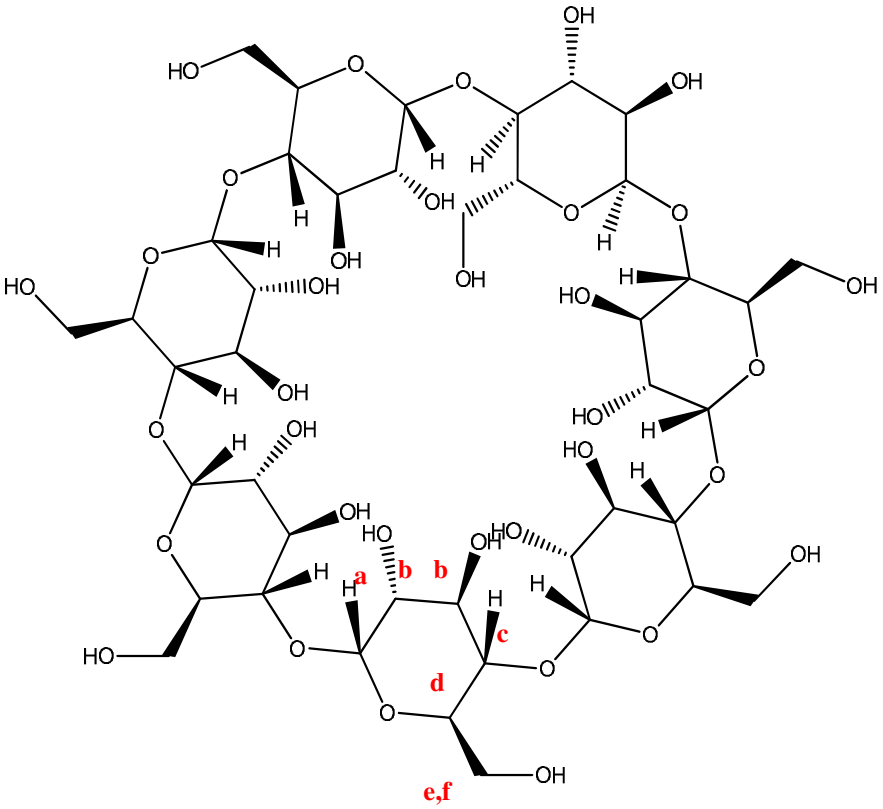

Structure 2. Structures of Th and βCD with labeled protons.

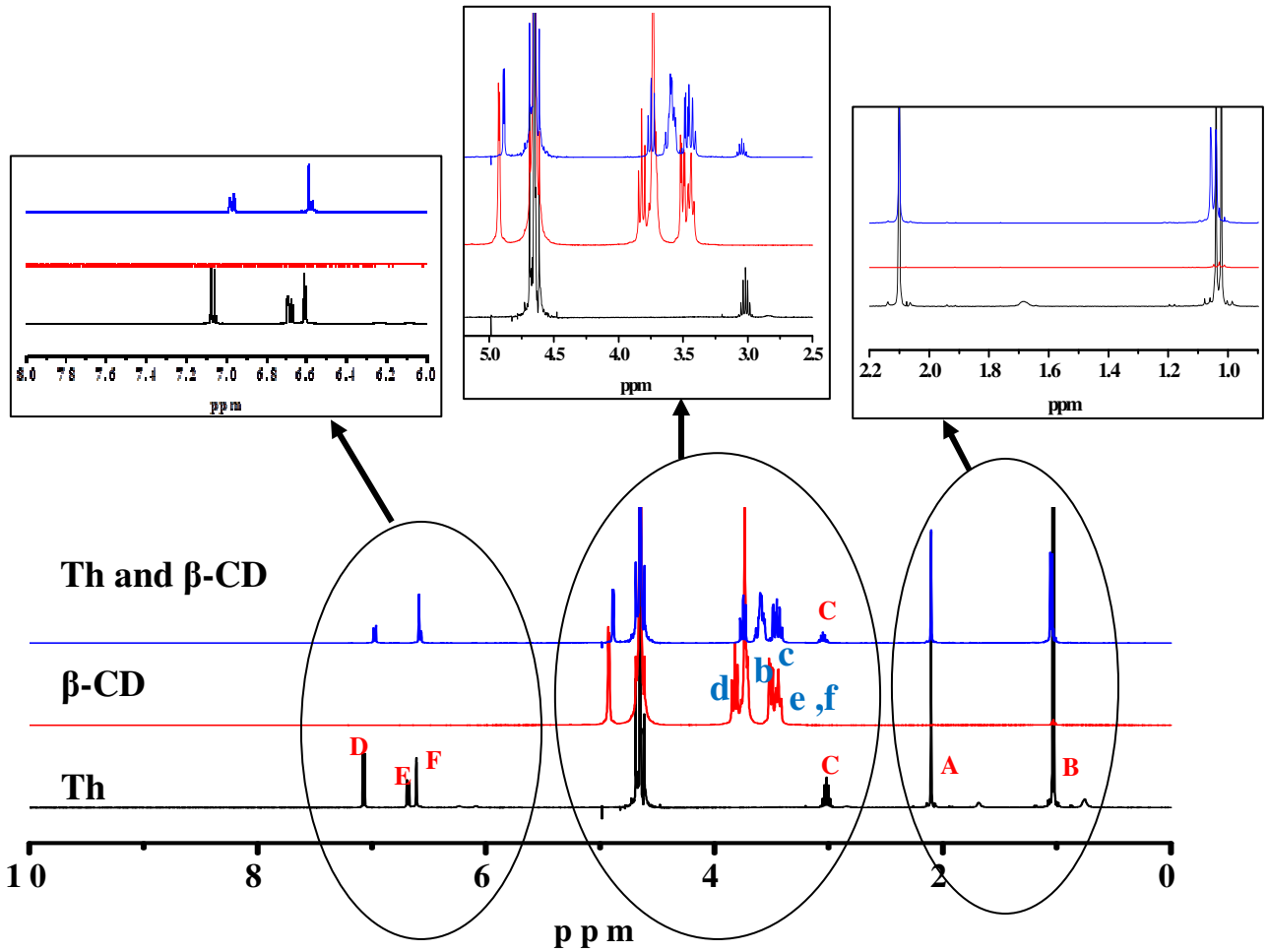

Fig. 9. ^{1}H-NMR spectra of Th in the absence and in the presence of βCD.

On the other hand ^{1}H NMR spectroscopic study of αCD and Th signifies a weaker interaction. Th aromatic protons have signals at 7.068 (D), 6.692 (E) and 6.612 (F) ppm and they remain unchanged after the addition of αCD. Also the protons of αCD remain

unchanged. This result suggested that thymol does not have influence in αCD environment, which is a signature of weaker interaction of Th in αCD.

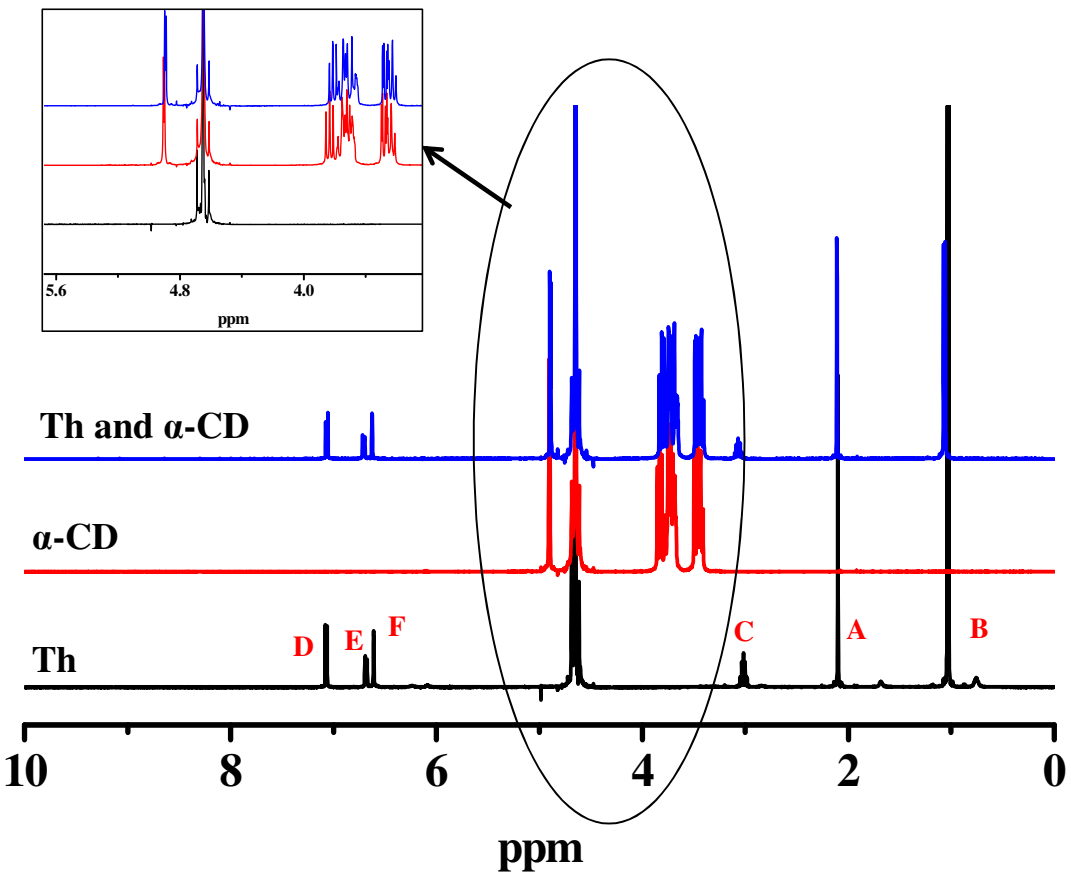

Fig. 10. ^{1}H-NMR spectra of Th in the absence and in the presence of αCD.

To explain the differential behavior of Th in the two CDs and the anomalous anisotropy behavior we have resorted to theoretical modelling studies.

3.7. Docking and simulation:

The two receptors, α and βCD differ in number of glucose residues (six in α, seven in βCD). They form a truncated cone shaped structure stiffened by hydrogen bonding around the outer rim. The cavities in two receptors have different diameters - 6.5 Å in αCD and 8.5 Å in βCD. The ligand, Th is planar with length ~7 Å. Docking results show that thymol can fit very well in the αCD with binding energy of -5.18 kcal/mole and to βCD with energy of -4.37 kcal/mole (fig. 11).

Docking results does not explain our experimental findings very well, since αCD has been experimentally found to discourage encapsulation of Th. But docking studies shows that the dimension of Th and αCD are appropriate for encapsulation. This lead us to consider a solvation sheath around Th molecules. From our previous communication we know that Th can behave as a photoacid,[14] hence, it remains in ionized state in its excited state which will result in a good hydration shell around Th. Again in ground state, chances of H-bonding and dipolar interaction can also result in similar hydration shell. This will effectively result in a bulkier Th approaching the CDs in every experimental cases. So this effect of hydration should be taken into account to understand the interaction. Hence, next we have resorted to some theoretical dynamics studies.

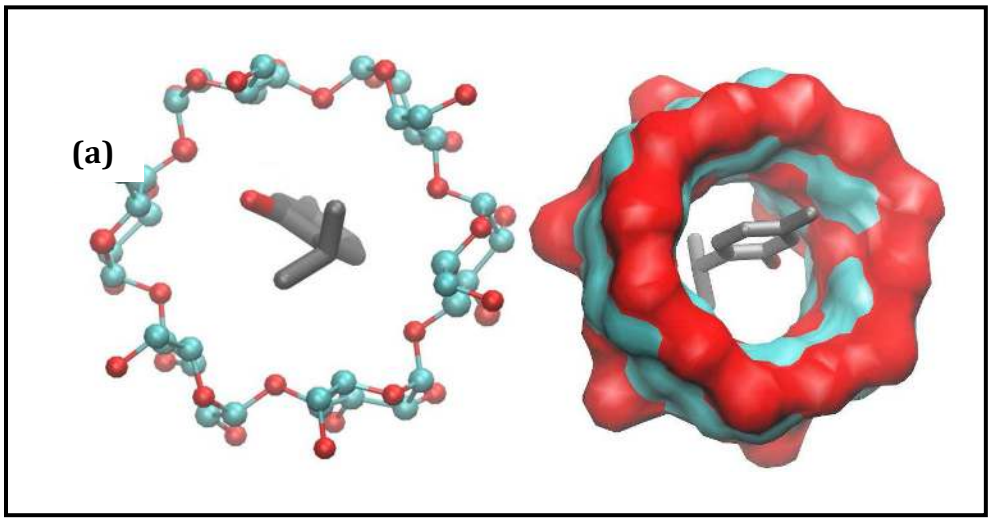

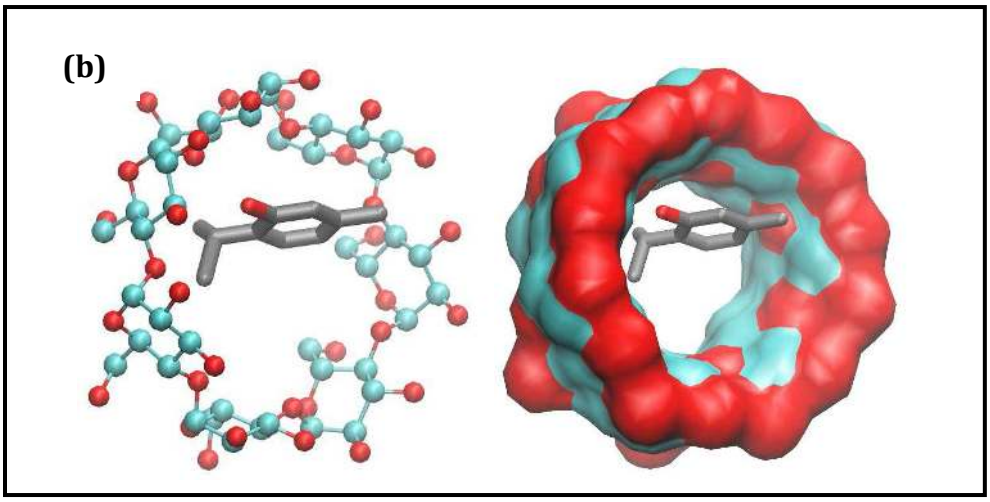

Fig. 11. Best docked pose of Th in (a) αCD, binding energy -5.18 Kcal/mole (b) βCD, binding energy -4.37 Kcal/mole.

3.8. Molecular Dynamics

Docking has several limitations such as the host backbones were considered rigid as well as the solvent effects were ignored. In the solution CDs becomes very flexible and both the hosts and guest forms hydrogen bonds with water, which affects the interaction dynamics with the guests. Therefore, both the host guest complexes were subjected to molecular dynamics (MD) simulation in aqueous environment for 48 ns. The whole simulation trajectories for αCD-Th and βCD-Th complexes can be visualized in videos S1 and S2 (online supporting information). The overall structural changes during the MD simulation, is shown in fig. 12 in terms of root mean square deviations (RMSD) with respect to the initial geometry. Fig. 12A shows that the fluctuations of Th overlaps with that of βCD, and gradually becomes more synchronized with the structural fluctuations of βCD suggesting the formation of a stable host-guest complex. On the other hand, Th was found to escape from the cavity of αCD after around 30 ns of simulation (fig. 12B and video S2) suggesting the unstable nature of Th-αCD complex.

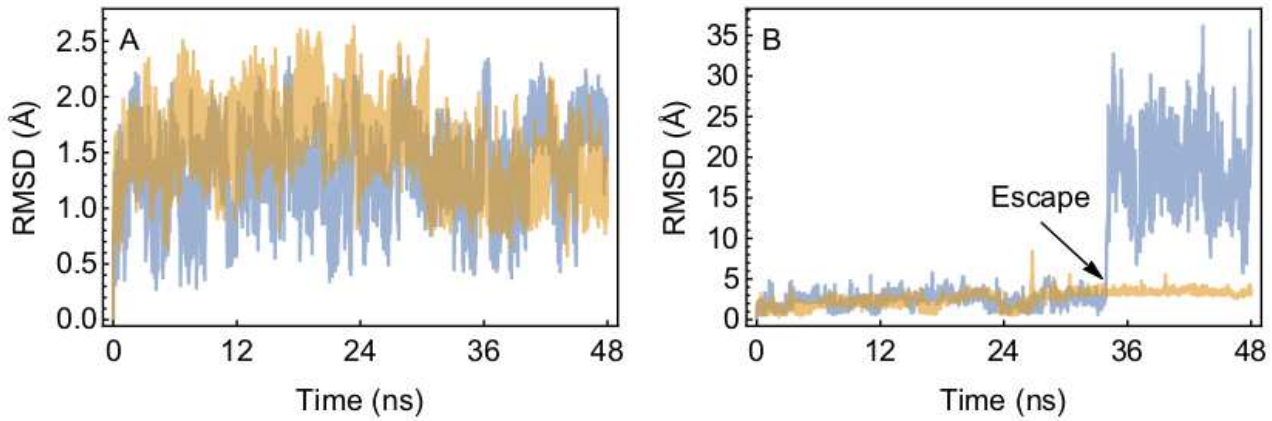

Fig. 12. RMSD of CD (brown) and Th (blue) in βCD-Th complex (A) and αCD-Th complex (B).

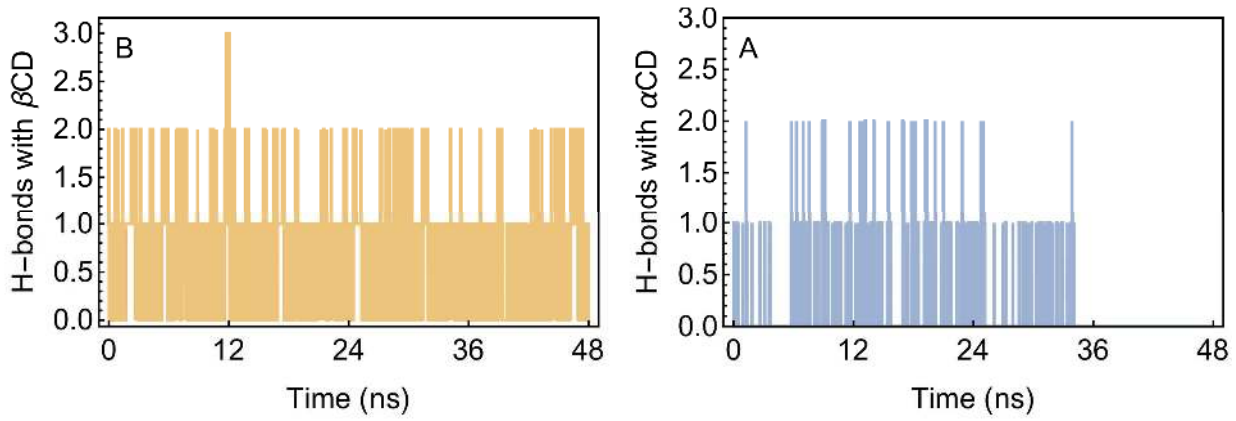

Fig. 13: Formation of split hydrogen bonds between Th and the OH groups of βCD (A) and αCD (B).

When we analyzed the trajectory for hydrogen bonding between Th and the OH groups of CDs, it was found that Th can form hydrogen bonds with both the CDs. However, the number of split hydrogen bonds and the frequency of formation of the hydrogen bonds were much less for αCD-Th complex than that was observed in βCD-Th complex (fig. 13). We also looked into the probable hydrogen bonding interactions of Th with solvent when in complex with CDs. The maximum number of split hydrogen bonds between Th and water at any given moment is shown in fig. 14A. A frequency distribution as shown in Fig. 14B suggesting that Th interacts more with water while complexed with αCD than in βCD, which could be the reason for its escape form the cavity of αCD into the solution.

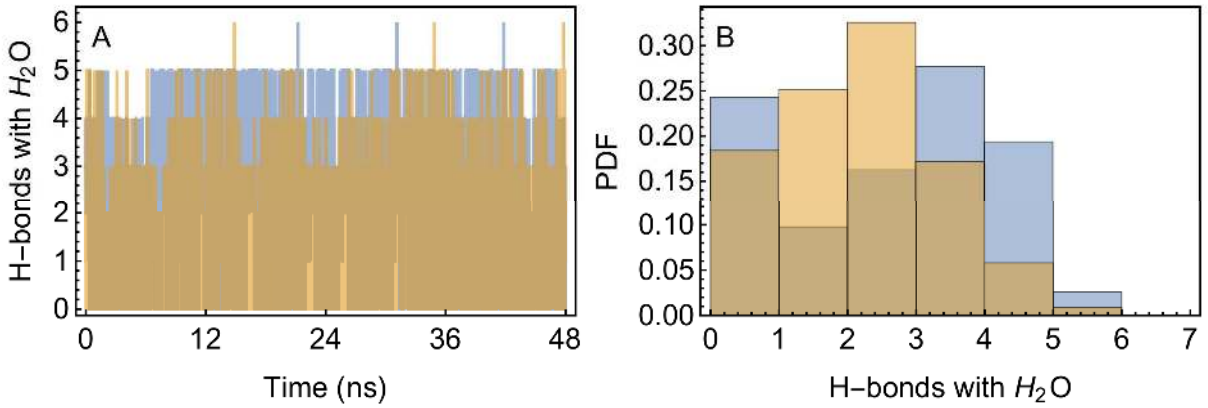

Fig. 14. Formation of split hydrogen bonds between Th and water when in complex with βCD (brown) and αCD (blue). (A) Hydrogen bonds at any given moment. (B) Frequency distribution.

3.9. Assay of DPPH radical scavenging activity of Th with αCD and βCD:

Thymol possesses excellent antioxidant properties due to the presence of phenolic hydroxyl group in its structure, which is known to exhibit potent antioxidant activity by absorbing and neutralizing free radicals.[28] In spite of the effective antioxidant activity at low concentrations *in vivo* and *in vitro*, thymol still sees a limited application in food industry due to its hydrophobicity that makes it difficult to uniformly disperse in food matrices. Encapsulation in micelles and cyclodextrins are standard methods to enhance solubilization. Micellar encapaulation and in vitro studies with Th has been already performed by Li Deng et al.[29] We have characterized encapsulated Th in CDs and have studied the change in its antioxidant and antibacterial behavior in encapsulated form.

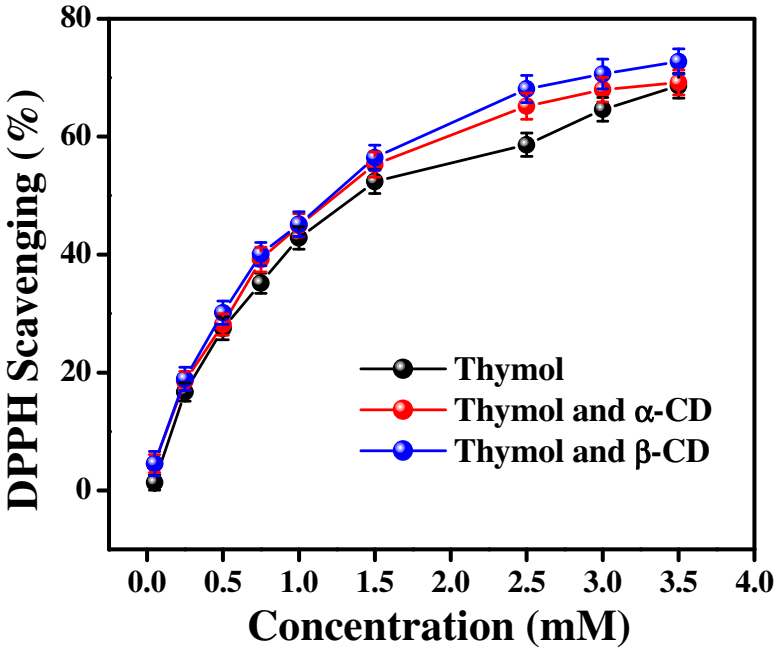

Fig. 15. Scavenging effects of free Th, Th-βCD and αCD complex on DPPH radical.

A cursory glance at fig. 15 points towards an improved antioxidant behavior of Th βCD complex, the improvement being more conspicuous from a βCD concentration above 1.5 mM. Hence this shows encapsulation of Th leads to an improvement of its antioxidant behavior.

4. Antimicrobial assay with *Bacillus subtilis:*

The antimicrobial activity of phenolic compounds is well-known. To screen the antimicrobial activity of unknown compounds the Agar diffusion assay (cylinder-plate method) is considered to be the simplest where the results are obtained rapidly. Inclusion

of Th into the cavity of α/βCD may be more beneficial than the free Th, since a bioactive individual component can change its properties in the presence of other compounds. In this context, we have performed the agar diffusion assay of Th at a concentration of 50 mg/ml and the result is represented in fig. 16. The formation of clear zones on the plates convincingly suggested about the inhibited growth of the test organism *B. subtilis* by Th. In addition, αCD had no significant effect on the activity of Thymol (fig. 16), whereas the effect of βCD was inconclusive (fig. 16).

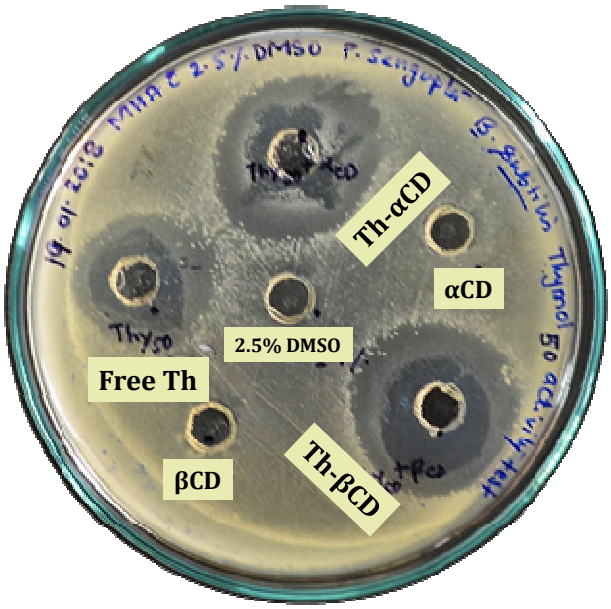

Fig. 16. Effect of Th, Th-αCD and Th-βCD on the growth of *B. subtilis* cells of Mueller Hinton agar plate.

5. Conclusion:

This work presents the encapsulation behavior of α and βCD on a small, biologically significant phenolic molecule Th. Fluorescence increment in case of βCD has demonstrated a facile encapsulation of Th whereas in αCD there was increment only in the initial stages. ITC data for βCD had also been in accordance to steady state and time resolved fluorescence and also NMR data. But surprisingly an expected increase in fluorescence anisotropy was not obtained. To explain this anomaly molecular docking and simulation experiments were conducted. And finally from a culmination of all data we were confirmed of an involvement of hydration sheath with Th which can dictate the extent of encapsulation of the molecule. βCD with a wider diameter can house Th better than smaller αCD. Finally we have also shown that encapsulation of Th within CD cavities does not hinder its biologically significant properties, namely, antioxidant and antibacterial behavior. Hence βCD can be safely employed as a delivery tool for Th in future research perspectives.

Acknowledgements:

AB gratefully acknowledges financial support of UGC for its project No. F 30-19/2014 (BSR), DST for its project No. YSS/2014/000403 and the FRPDF grant from Presidency University. The authors are also grateful to Dr. Pinki Saha Sardar of Bhawanipur Education Society College for lifetime experiments. AB wants to thank Prof. Nikhil Guchhait of Calcutta University for his useful suggestions, Prof. Gopal Chakraborty of Calcutta

University for the ITC instrument (DBT IPLS Maintenance Fund). AB also wants to thank Prof. Abhijit Chakraborty, Prof. Samita Basu and Ms. Chaitrali Sengupta of Saha Institute of Nuclear Physics for the anisotropy and theoretical modelling measurements. AB and PS want to thank Mr. Tapendu Samanta, Mr. Prasenjit Mondal, and Mr. Chhandak Adhikary for their help during experiments. PS thanks WBDST, West Bengal for her fellowship (Project no. 546(sanc.)/ST/P/S&T/4G-13/2014).

References:

1. W. Seanger, *Angew. Chem. Int. Ed. Engl.*, 1980, 19, 344-362.
2. J. Szejtli, *Chem. Rev*., 1998, 98, 1743–1754.
3. J. M. Schuette, T. T. Ndou, A. M. de la Pena, S. Mukundan Jr., I. M. Warner, *J. Am. Chem. Soc.*, 1993, 115, 292-298.
4. J. van Stan, S. De Feyter, F. C. De Schrywer, C. H. Evans, *J. Phys. Chem*., 1996, 100, 19959-19966
5. G. Gonzales-Gaitano, A. Compostizo, L. Sanchez-Martin, G. Tardajos, *Langmuir*, 1997, 13, 2235-2241.
6. K. B. Lipkowitz, S. Raghothama, J. Yang, *J. Am. Chem. Soc*., 1992, 114, 1554-1562.

7. Y. Inoue, K. Yamamoto, T. Wada, S. Everitt, X.-M. Gao, Z.-J. Hou, L.-H. Tong, S.-K. Jiang, H.-M. Wu, *J. Chem. Soc., Perkin Trans*., 1998, 2, 1807-1816.
8. A. Tsortos, K. Yannakopulou, K. Eliadu, I. M. Mavridis, G. Nouniesis, *J. Phys. Chem. B*, 2001, 105, 2664-2671.
9. V. T. De Sousa, K. B. Lipkowitz (Eds.), *Chem. Rev*., 1998, 98, 1741-1742.
10. R. L. Carrier, L. A. Miller, I. Ahmed, *J. Controlled Release*, 2007, 123, 78-99.
11. T. Loftsson, M. E. Brewster, M. Masson, *Am. J. Drug Deliv.,* 2004, 2, 261–275.
12. C. F. Bagamboula, M. Uyttendaele, J. Debevere, *Food Microbiology*, 2004, 21, 33-42.
13. N. V. Yanishlievaa, E. M. Marinovaa, M. H. Gordonb, V. G. Ranevaa, *Food Chemistry*, 1999, 64, 59-66.
14. A. Bose, D. Parbat, M. Mukherjee, P. S. Sardar, S. Ghosh, *Spec. let.,* 2017, 50, 81-87.
15. H. A. Benesi, J. H. Hildebrand, *J. Am. Chem. Soc*., 1949, 71, 2703-2707.
16. J. R. Lakowicz, Principles of Fluorescence Spectroscopy, third ed., Plenum, New York, 2006.
17. K. J. Bowers, E. Chow, H. Xu, R. O. Dror, M. P. Eastwood, B. A. Gregersen, J. L. Klepeis, I. Kolossvary, M. A. Moraes, F. D. Sacerdoti, J. K. Salmon, Y. Shan, D. E. Shaw, (2006). Scalable Algorithms for Molecular Dynamics Simulations on Commodity Clusters. In Proceedings of the ACM/IEEE SC 2006 Conference, pp. 43–43.
18. J. L, Banks, H. S. Beard, Y. Cao, A. E. Cho, W. Damm, R. Farid, A. K. Felts, T. A. Halgren, D. T. Mainz, J. R. Maple, R. Murphy, D. M. Philipp, M. P. Repasky, L. Y. Zhang, B. J. Berne, R. A. Friesner, E. Gallicchio, R. M. Levy, *J. Comput. Chem*., 2005, *26*, 1752–1780.

19. U. Pal, S. K. Pramanik, B. Bhattacharya, B. Banerji, N. C. Maiti, *Springer Plus*, 2016, 5, 1121-1138.

20. K., Shimada, K., Fujikawa, K., Yahara, & T. Nakamura, *J. Agric. and Food Chem*., 1992, 40, 945–948.

21. J. H. Mueller and J. Hinton, *Exp. Biol. Med*., 1941, 48, 330-333.

22. M. A. Wikler, F. R. Cockerill, K. Bush, M. N. Dudley, G. M. Eliopoulos, D. J. Hardy, D. W. Hecht, M. J. Ferraro, J. M. Swenson, J. F. Hindler, J. B. Patel, M. Powell, J. D. Turnidge, M. P. Weinstein, B. L. Zimmer, Performance Standards for Antimicrobial Disk Susceptibility Tests; Approved Standard—Tenth Edition, Clinical and Laboratory Standards Institute, 2009.

23. H. Takakusa, K. Kikuchi, Y. Urano, T. Higuchi, and T. Nagano, *Anal. Chem*., 2001, 73, 939-942.

24. A. Samanta, N. Guchhait, S. C. Bhattacharya, *J. Phys. Chem. B*, 2014, 118, 13279–13289.

25. P.D. Ross and S. Subramanian, *Biochemistry*, 1981, 20, 3096-3102.

26. E. Leyva, E. Moctezuma, J. Strouse, M. A. Garciagaribay; *J. Incl. Pheno. Macro. Chem*. 2001, 39**,** 41–46.

27. R. Zhao, C. Sandström, H. Zhang, T. Tan, *Molecules*, 2016, 21, 372-382.

28. S. Venu, D. B. Naik, S. K. Sarkar, U. K. Aravind, A. Nijamudheen, C. T. Aravindakumar, *J. Phys. Chem. A*, 2013, 117**,** 291–299.

29. L.-Li Deng, M. Taxipalati, F. Que, H. Zhang, *Scientific reports*, 2016, 6, 38160-38167.

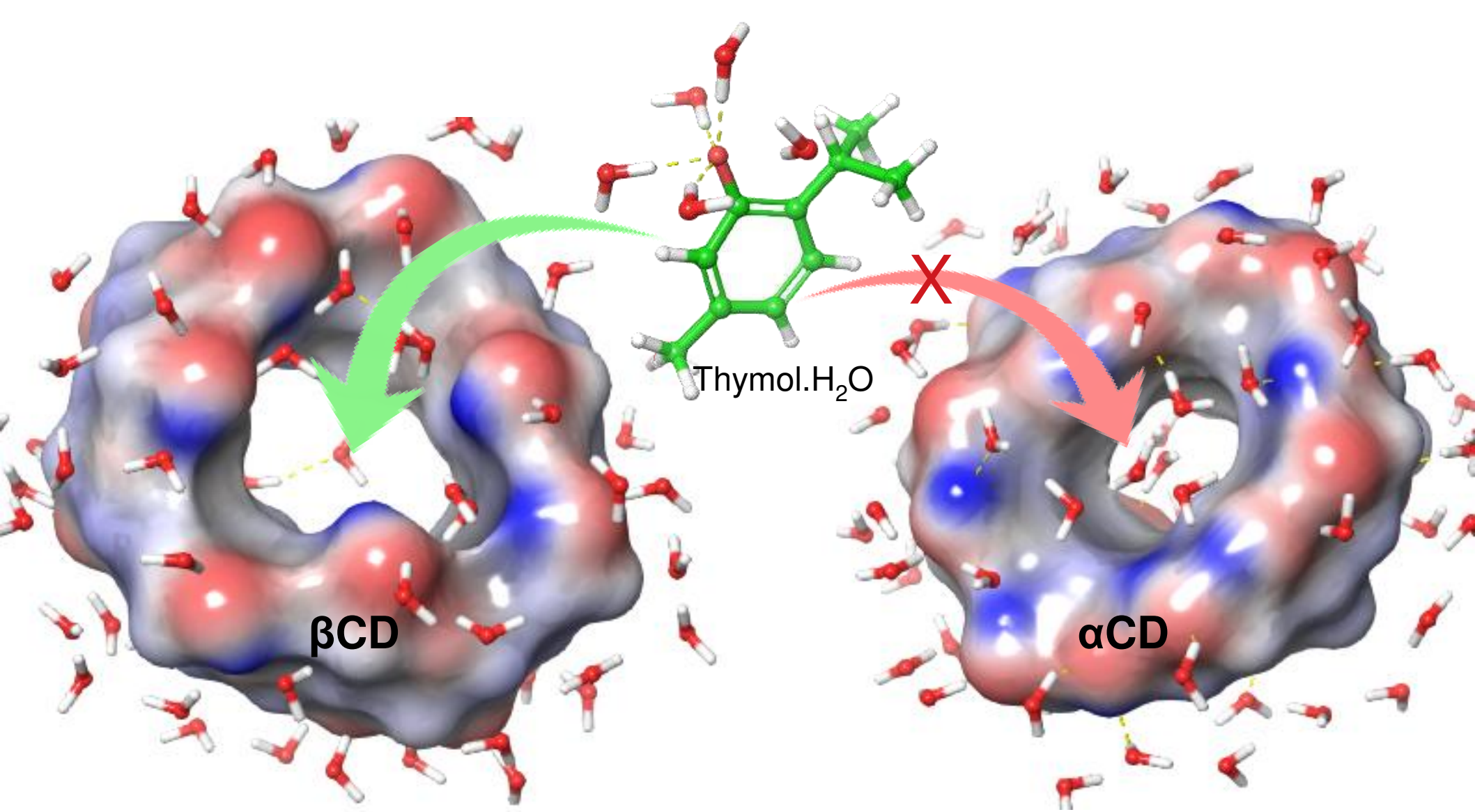
Thymol.H2O
βCD
αCD